Food Packaging and Shelf Life 36 (2023) 101046

Contents lists available at ScienceDirect

Food Packaging and Shelf Life

journal homepage: www.elsevier.com/locate/fpsl

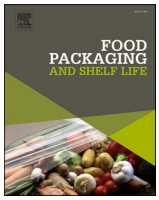

Biodegradable fish gelatin/chitosan-based active films alter chill-stored golden pomfret (*Trachinotus blochii*) metabolites mainly through modulating four metabolic pathways

Yi Liu [a,b], Yi Kai [a], Hongshun Yang [a,b,*]

[a] Department of Food Science & Technology, National University of Singapore, 117542, Singapore
[b] National University of Singapore (Suzhou) Research Institute, 377 Lin Quan Street, Suzhou Industrial Park, Suzhou, Jiangsu 215123, PR China

ARTICLE INFO

Keywords:
Active packaging
Biodegradable film
Essential oil
Alpha-tocopherol
Metabolomics
Fish preservation

ABSTRACT

The high perishability of fish after capture requires effective preservative strategies to delay its quality loss and extend shelf-life of fish products during chilled storage. There has been a growing interest in employing biodegradable active films for chill-stored fish preservation due to the increasing environmental concern of plastic packaging disposal. The aims of this work were to develop fish gelatin/chitosan-based films loaded with nanoemulsified α-tocopherol (α-TP) and thyme essential oil (TEO) and their combination, and to evaluate the effectiveness of the films to inhibit fish quality deterioration. Nanoemulsified biopreservatives were obtained by ultrasonication with desirable polydispersity index. A good compatibility of the nanoemulsions within the film matrix was observed using confocal laser scanning microscopy (CLSM) and their uniform distribution rendered the active films compact and smooth surface morphology as revealed by SEM. FTIR spectra showed that the chemical structure of the films was altered by incorporation of the natural materials. For metabolic profiles in chill-stored fish fillets, totally 47 metabolites were identified using NMR spectroscopy. Amino acid metabolism was found to be the most influenced pathway during fish storage. Besides, the production of some undesirable metabolites such as organic acids, putrescine, tyramine, and hypoxanthine were markedly reduced, which suggested that the active packaging could preserve fish quality through interfering the carbohydrate, nitrogen, and nucleotide metabolisms. Combination of nanoemulsified α-TP and TEO extended the fish shelf-life to 15 days with TVB-N values under the rejection limit, which further confirmed that the biodegradable active films could effectively delay fish quality deterioration.

1. Introduction

With the rising apprehensions regarding the serious ecological accumulation problems resulting from the excessive usage of nonbiodegradable petroleum-based synthetic plastics (Tessaro et al., 2021; Yang et al., 2019), biodegradable films made from naturally sourced biopolymers, mainly proteins and polysaccharides, have been the research focus in recent decades as promising alternatives to the plastics of synthetic origin (Gulzar et al., 2022; Kumar et al., 2018; Martins et al., 2012; Pérez-Córdoba et al., 2018; Tessaro et al., 2021; Yadav et al., 2020). Their application in food industry not only helps deal with environmental concerns caused by the accumulation of plastic waste but protects consumers from exposure to the styrene monomer and plasticizers that may migrate from packaging materials into foods (Pilevar et al., 2019). Moreover, these biopolymer-based films can serve as active packaging to keep the food quality during storage and extend the shelf life of food products, by acting as excellent vehicles for delivery of incorporated bioactive compounds and providing them with a controlled release during the required time (Bahrami et al., 2020; Wu et al., 2022).

Within biopolymers, gelatin and chitosan have been recognized as promising excipients for fabrication of biopolymer-based films due to their advantageous characteristics, such as biocompatibility, biodegradability, non-toxicity, and film-forming ability (Kanatt et al., 2012; Yadav et al., 2020). Development and characterization of biodegradable gelatin/chitosan-based active films have been extensively reported in recent years (Bonilla et al., 2018; Haghighi, De Leo, et al., 2019; Li et al., 2021; Roy & Rhim, 2021; Wu et al., 2014; Yadav et al., 2020).

* Corresponding author at: Department of Food Science and Technology, National University of Singapore, 117542, Singapore.
E-mail address: fstynghs@nus.edu.sg (H. Yang).

https://doi.org/10.1016/j.fpsl.2023.101046
Received 18 October 2022; Received in revised form 27 January 2023; Accepted 29 January 2023
Available online 11 February 2023

Combination of chitosan and gelatin as film-forming solutions renders bio-composite films enhanced mechanical robustness and barrier properties against environmental stress such as oxygen and light (Pérez Córdoba & Sobral, 2017), owing to formation of polyelectrolyte complexes between positively charged chitosan and negatively charged gelatin, along with production of strong hydrogen bond (Haghighi, De Leo, et al., 2019; Wang et al., 2021). Besides, the intrinsic antimicrobial character of chitosan promises the films as active packaging for protection of food products from biological alterations over time (Bahrami et al., 2020). The incorporation of bioactive agents into the bio-composite films could further extend their functional properties such as antimicrobial and antioxidant properties.

More recently, with increasing demands of consumers for organic and safer food products, natural bioactive substances such as essential oils with potent antimicrobial and antioxidant activities are emerging in food packaging (Bahrami et al., 2020; Martins et al., 2012; Bhowmik et al., 2022; Roy, et al., 2021; Yemmireddy et al., 2020). Although some studies have reported that gelatin/chitosan-based films could serve as effective carriers for those functional ingredients over fish spoilage and quality deterioration of fresh-cut fruits (Gómez-Estaca et al., 2010; Kakaei & Shahbazi, 2016; Zhang, Yang, et al., 2021), potential applications of gelatin/chitosan-based films as active packaging are still limited in the realm of food biopreservation and the underlying preservative mechanisms have yet to be elucidated especially on the molecular level.

Therefore, the objectives of this study were to develop biodegradable fish gelatin/chitosan-based films loaded with nanoemulsified active compounds (thyme essential oil, α-tocopherol, and their combination) by casting technique, and to evaluate the effects of these functional substances on their microstructure and physicochemical properties. Furthermore, the bio-composite active films were used as active packaging to preserve the chill-stored golden pomfret fillets, and the relationship between metabolite profiles and fish quality over time was uncovered by high resolution NMR spectroscopy coupled with multivariate analysis.

2. Materials and methods

2.1. Materials

Commercial fish gelatin (FG) was kindly provided by Yiweilong Biological Technology Co., Ltd (Xiamen, Fujian, China). Corn oil was purchased from FairPrice (Singapore). Food-grade thyme (*Thymus vulgaris*) essential oil (TEO), α-tocopherol (α-TP), chitosan (CS, 75–85% deacetylation degree, Mw 50–190 kDa), glycerol, Tween® 80, and fluorescent dyes (Nile Red and Nile Blue A) were obtained from Sigma-Aldrich (St. Louis, MO, USA). Other chemical reagents were of analytical grade.

2.2. Nanoemulsion preparation

The nanoemulsions encapsulating α-TP and/or TEO were prepared according to Chang et al. (2012) with some modifications. The oil phase (10%, w/w) composed of fixed amounts of active compounds (α-TP or TEO) (3%, w/w), or their combination (6%, w/w) and corn oil as ripening inhibitor was mixed with Tween® 80 (1%, w/w), and deionized (DI) water (89%, w/w) using a high-speed blender (F6/10, Jingxin, Shanghai, China) at 15,000 rpm for 2 min. The coarse emulsions were then sonicated on ice with an ultrasonic homogenizer (JY92-IIN, SCIENTZ, Ningbo, China) fitted with a 2-mm diameter of titanium probe at a power level of 300 W for 5 min (on-time: 3.0 s; off-time: 3.0 s). The oil-in-water nanoemulsion without active compounds was also prepared as control.

After preparation, the mean droplet size and polydispersity index (PDI) of the nanoemulsions were determined using a dynamic light scattering (DLS) device (Nano Brook Omni, Brookhaven instruments, USA) at a fixed scattering angle of 173°. The nanoemulsion specimens were diluted 100 times with DI water before analysis to avoid multiple scattering effects. Each measurement was performed in triplicate.

2.3. Film production

Biodegradable films were produced by casting technique (Bonilla et al., 2018; Pérez Córdoba, et al., 2017). Briefly, film-forming solutions (FFS) were prepared by thoroughly mixing aliquots of FG (4 g/100 mL of DI water) and CS (1 g/100 mL of aqueous solution of glacial acetic acid (1%)), nanoemulsified active compounds (5 g/100 g biopolymer), and glycerol (30 g/100 g biopolymer) as a plasticizer with gently stirring for 10 min, and subsequently homogenized using a high-speed blender (F6/10, Jingxin, Shanghai, China) at 10,000 rpm for 5 min. During stirring, the pH was adjusted to 5.6 to obtain the polyelectrolyte complexes between FG and CS, which can only form at a selected pH above the isoelectric point of FG (PI=4.5–5.2) to be negatively charged, and below the pKa of the amino group (pH=6.2–6.5) of CS to be positively charged, as well as to avoid any phase separation (Benbettaïeb et al., 2015; Pérez-Córdoba et al., 2018). After degassing, the FFS were cast in plate dishes (15 cm diameter), and then dried in a controlled environment chamber (KBF 240 Binder, ODIL, France) at 37 ℃ for 36 h. After peeling, five different types of films were obtained: (N0) FG/CS-based films (without nanoemulsions); (N1) FG/CS-based films loaded with nanoemulsions (without active compounds); (N2) FG/CS-based films loaded with nanoemulsified α-TP; (N3) FG/CS-based films loaded with nanoemulsified TEO; (N4) FG/CS-based films loaded with nanoemulsified α-TP and TEO.

2.4. Film characterization

2.4.1. Water solubility

Film samples measuring 1 cm^2 were immersed in 15 mL of DI water with gently stirring at room temperature for 24 h. After that, the undissolved film samples were recovered and dried at 105 ℃ for 24 h. Water solubility (%) was expressed as g of solubilized film (dry matter)/100 g of desiccated film samples (Gómez-Estaca et al., 2010).

2.4.2. Fourier transformed infrared (FTIR) analysis

The chemical structure of film samples was measured by Spectrum One FTIR spectrometer (PerkinElmer, Waltham, MA, USA) within a wavelength range of 4000–400 cm^{-1} at a resolution of 4 cm^{-1} and 64 scans. Prior to FTIR analysis, film samples were conditioned at 0% RH.

2.4.3. Confocal laser scanning microscopy (CLSM)

The microstructure of the film samples was measured with Zeiss LSM710 confocal laser scanning microscope (Carl Zeiss Inc., Braunschweig, Germany). The dual-dyed film samples were prepared by mixing the fluorescent dye solution (composed of Nile Red and Nile Blue A) with FFS at a concentration of 0.04 g/kg (Liu et al., 2019). Observation of the stained samples was made by excitation of Nile Blue A at 633 nm and Nile Red at 488 nm, respectively.

2.4.4. Scanning electron microscopy (SEM)

A field emission scanning electron microscopy (FESEM, JEOL JSM-6701 F, Tokyo, Japan) was used to investigate the surface morphology of the dried film samples (Zhang, Yang, et al., 2021). The film to observe its microstructure was mounted on specimen holders before coated with a gold layer. SEM images of film samples were observed at an accelerating voltage of 5.0 kV.

2.5. Fish storage trial

Golden pomfret (*Trachinotus blochii*) was purchased from Sheng Siong Supermarket (Singapore). After deboning and evisceration, the fish fillets were pieced, film packaged, and divided into five groups: (I)

golden pomfret fillets with no film wrapping; (II) golden pomfret fillets wrapped with film N1; (III) golden pomfret fillets wrapped with film N2; (IV) golden pomfret fillets wrapped with film N3; and (V) golden pomfret fillets wrapped with film N4. The fish fillets were then packed in sterile polyethylene bags and stored at 4 ℃ for 15 days for further analysis.

2.6. Determination of total volatile basic nitrogen (TVB-N)

The fish fillets were homogenized with DI water at a ratio of 1:10 (w/v), and then centrifuged at 10,000 ×*g* for 5 min at 4 ℃ to obtain the supernatant for determination of TVB-N value (Cen et al., 2021).

2.7. Metabolite extraction

Metabolite extraction from golden pomfret fillets was carried out as described by Zhao et al. (2019) with some modifications. Briefly, two grams of fish samples were homogenized with 5 mL of methanol: water (2:1, v/v) for 5 min, and further ultrasonicated on ice for 5 min. The homogenates were centrifuged at 12,000 ×*g* for 10 min at 4 ℃ and the obtained supernatant was then subjected to freeze-drying for methanol removal (Wang et al., 2019). The extracted metabolites were redissolved in 600 μL of deuterium water (D_2O, 99.9%) containing 0.01% (w/v) of 3-trimethylsilyl [2,2,3,3-d_4] propionate (TSP, Sigma-Aldrich, St Louis, MO, USA) as an internal reference. After centrifugation at 12,000 ×*g* for 10 min at 4 ℃, 550 μL of the resulting supernatant was immediately pipetted into a 5-mm NMR tube for NMR analysis.

2.8. NMR spectroscopy

The extracted metabolites were analysed at 25 ℃ using a Bruker DRX-500 NMR spectrometer (Bruker, Rheinstetten, Germany) fitted with a Triple Inverse Gradient probe at 500.23 MHz. The ^{1}H spectra were acquired using the standard Bruker NOESY pulse sequence (noesypr1d) with an acquisition time of 3.3 s, 128 scans, and a relaxation delay of 2 s. A 90° pulse length of each sample was modified using the automatic pulse calculation (pulsecal) in TopSpin 4.1.4 (Bruker, Rheinstetten, Germany). The free induction decays were multiplied by an exponential function equivalent to 1 Hz line broadening factor before Fourier transformation. The 2D ^{1}H–^{13}C heteronuclear single quantum coherence spectroscopy (HSQC) was also performed at 25 ℃ for metabolite identification. With the Bruker hsqcedetgpsisp2.3 pulse sequence applied, the ^{1}H spectra with a 10-ppm spectrum width and the ^{13}C spectra with a 165-ppm spectrum width were collected in the F2 and F1 channels, respectively (Zhao et al., 2020).

2.9. NMR spectra processing and data analysis

The NMR spectra of each sample were automatically adjusted for phase and baseline correction with TopSpin 4.1.4 (Bruker, Rheinstetten, Germany). Afterwards, the metabolites were identified referring to the Human Metabolome Database (https://hmdb.ca/) and some related references (Locci et al., 2011; Shumilina et al., 2015), and quantified by automatic referencing of TSP integrals for further analysis (Jégou et al., 2015).

For multivariate analysis, the ^{1}H spectra were processed and standardised using Mestrenova (Mestreab Research SL, Santiago de Compostela, Spain). The binned data were then analysed with principal component analysis (PCA) for group separation and orthogonal projection to latent structures-discriminant analysis (OPLS-DA) to identify the dissimilarities among treatments with SIMCA (version 14.1, Umetrics, Umeå, Sweden). The identified metabolites with VIP > 1 were applied for volcano plots, among which those with FCs > 2.0 (or FCs < 0.5) and $P < 0.05$ were considered statistically significant (Shen et al., 2018). Moreover, the crucial pathways were identified based on the database MetaboAnalyst 5.0 (https://www.metaboanalyst.ca/).

2.10. Statistical analysis

Analysis of variance (ANOVA) was performed with SPSS Statistics (IBM Corp., Armonk, NY, USA), and differences between multiple means of treatments were determined by Duncan's multiple range test at $P < 0.05$.

3. Results and discussion

3.1. Characteristics of the nanoemulsions

Droplet size and PDI values, which are two important physical characteristics of an emulsion that could effectively affect the stability of colloidal system, were measured in our study. The nanoemulsions without active compounds encapsulated (control) had the mean droplet size of around 260 nm, which exhibited no significant difference from those with α-TP encapsulated, whereas incorporation of TEO significantly decreased the size to about 200 nm (Table 1). Besides, PDI value is a measure for the broadness of droplet size distribution varying from 0 to 1, and the closer the PDI value to 1, the broader distribution it represents (Sharif et al., 2017). All nanoemulsions produced in our study were found to possess a monomodal size distribution with PDI values lower than 0.30, which indicated the superior stability and uniformity of the nanoemulsions (Zhang, Yang, et al., 2021). Similar results were also reported that incorporation of α-TP with certain active compounds (namely, garlic oil and cinnamaldehyde) rendered a uniform droplet size distribution and desired physical stability during the 90-day storage period (Pérez-Córdoba et al., 2018). The narrow intensity peak (Fig. S1 in Supplementary Material) and relatively low PDI value of the nanoemulsions confirmed the efficiency of the ultrasonication method in the production of uniform nanoemulsions.

3.2. Characteristics of the biodegradable active films

3.2.1. Water solubility

The film solubility in water (FS) is an essential physical property that can largely determine the release of encapsulated active compounds and thus their functional attributes such as antimicrobial and antioxidant activities for food preservation when applied to food surface (Gómez-Estaca et al., 2010). In our study, film N0 (without nanoemulsions) showed the highest FS value (65.1 ± 0.8%), and no significant difference ($P > 0.05$) was observed as compared to film N3 (loaded with TEO nanoemulsion (Fig. 1A). However, incorporation of nanoemulsified α-TP into the FG/CS-based films sharply reduced the FS value to 9.8 ± 0.0% for film N2 and 40.9 ± 2.5% for film N4, respectively, which could be ascribed to the hydrophobic nature of α-TP. Besides, compared to film N0, the lower FS value (41.0 ± 1.1%) of film N1 could be attributable to the presence of the oil phase in the film matrix, which

Table 1
Mean droplet size and polydispersity index (PDI) of freshly prepared nanoemulsions loaded with *α*-tocopherol and/or thyme essential oil.

Samples	Droplet size (nm)	PDI
NEs	258.9 ± 1.1^a	0.30 ± 0.00^a
α-TP NEs	263.8 ± 7.4^a	0.24 ± 0.02^c
TEO NEs	198.6 ± 1.8^b	0.27 ± 0.02^b
α-TP/TEO NEs	260.3 ± 3.3^a	0.27 ± 0.01^b

Mean values ± standard deviation (n = 3). Means with different lowercase letters in the same column indicate significant differences ($p < 0.05$) among different nanoemulsion samples.
α-TP: *α*-tocopherol; TEO: thyme essential oil.
NEs: nanoemulsions encapsulating no active compounds (Control); *α*-TP NEs: nanoemulsions encapsulating *α*-tocopherol; TEO NEs: nanoemulsions encapsulating thyme essential oil; *α*-TP/TEO NEs: nanoemulsions encapsulating *α*-tocopherol and thyme essential oil.

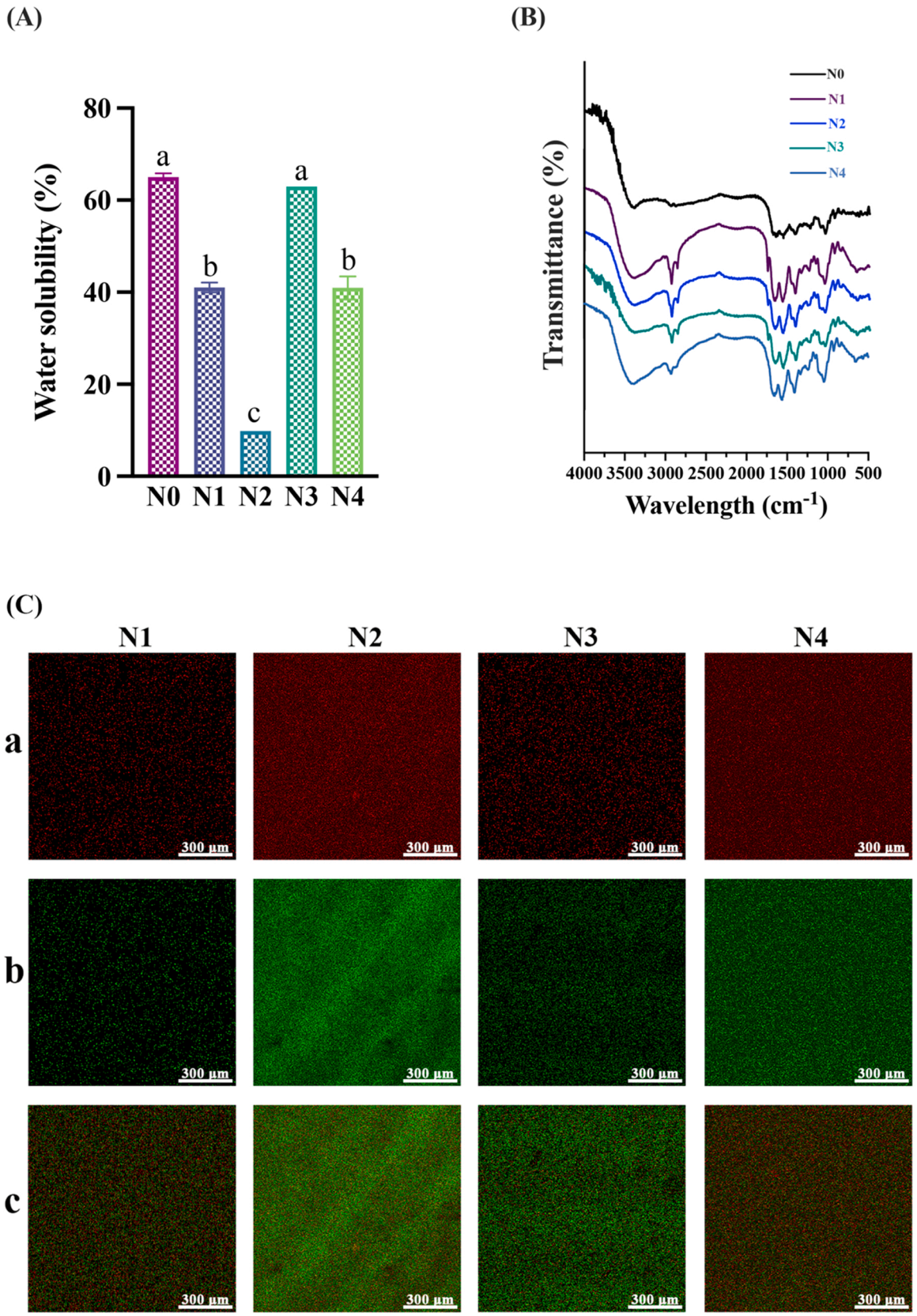

Fig. 1. Water solubility (A), FTIR spectra (B), and CLSM (C) images of fish gelatin/chitosan-based (FG/CS-based) films. (N0) FG/CS-based films (without nanoemulsions); (N1) FG/CS-based films loaded with nanoemulsions (without active compounds); (N2) FG/CS-based films loaded with nanoemulsified α-tocopherol; (N3) FG/CS-based films loaded with nanoemulsified thyme essential oil; (N4) FG/CS-based films loaded with nanoemulsified α-tocopherol and thyme essential oil. Means with different lowercase letters are significantly different among different film samples ($P < 0.05$). (a) Excitation at 633 nm in red; (b) Excitation at 488 nm in green; (c) Combined image of (a) and (b).

may reduce the film hydrophilicity (Tessaro et al., 2021).

3.2.2. Fourier transformed infrared (FTIR) spectroscopy

The FTIR spectra of biodegradable FG/CS-based films loaded with nanoemulsified active compounds are shown in Fig. 1B. The broad bands in the range of 3600–3200 cm^{-1} were characteristic of O-H stretching vibration that overlapped with N-H stretching within the same region. The bands between 3000 and 2800 cm^{-1} could be assigned to vibration of the C-H stretching, among which peaks at 2926 and 2855 cm^{-1} were indicative of the presence of symmetric and antisymmetric -CH_2 groups (Chen et al., 2016; Pérez Córdoba, et al., 2017). Moreover, the bands at 1646 cm^{-1}, 1562 cm^{-1}, and 1238 cm^{-1} indicated carbonyl (C═O) stretches, N-H amide bending vibration, and C-N stretching, respectively (Pereda et al., 2011; Pérez Córdoba, et al., 2017).

Incorporation of nanoemulsions generated a tiny new band at peak of 1746 cm^{-1}, which may represent the C═O stretching of fatty acid esters present in corn oil (used as ripening inhibitor in the nanoemulsions). Tessaro et al. (2021) also reported a tiny peak at 1744 cm^{-1} present in bovine gelatin-chitosan films incorporated with a double emulsion (W/O/W). Besides, the FTIR spectra of FG/CS-based films loaded with active compounds (α-TP and/or TEO) showed a slight shift at some existing peaks (e.g., at 3377 cm^{-1} and 1047 cm^{-1}), evidencing the appearance of these active compounds in the film matrix. Specifically, bands at around 1047 cm^{-1} could be manifested by the stretching vibration of C-O-H bond, and its hydration was reported to be positively correlated with water absorption ability of chitosan-based films (Martins et al., 2012).

3.2.3. CLSM & SEM

The spatial arrangement of the nanoemulsions in the film matrix could contribute to the film morphology and other properties such as mechanical properties and water solubility (Nisar et al., 2018). To reveal the distribution of the nanoemulsion droplets in film samples, a dual fluorescent dye solution composed of Nile Red and Nile Blue A was applied to stain the oil phase and the continuous biopolymer phase, respectively. As shown in Fig. 1 C, the nanoemulsion droplets exhibited a homogeneous distribution within the film matrix (films N1-N4), among which films N2 and N4 loaded with nanoemulsified α-TP distinctly featured more oil droplets that were more uniformly distributed than those in films N1 and N3. The uniform droplet distribution observed in CLSM images was consistent with the narrow intensity peak of the nanoemulsions shown in Fig. S1 (Supplementary Material), as well as their relevant PDI values (Table 1). It could be ascribed to the polyelectrolyte complexes formed between FG and CS that served as an emulsifier, hindering the dispersed oil droplets from flocculation and coalescence, thus leading to the good stability and uniform distribution of the nanoemulsions in the biopolymer-based films (Liu et al., 2019).

SEM was used to image the surface topography of biodegradable FG/CS-based active films and to study the microstructural changes in the biopolymer films loaded with various bioactive compounds (Fig. S2 in Supplementary Material). All the five bio-based films totally exhibited a compact, smooth, and homogeneous surface structures without any large pores present, although incorporation of nanoemulsified α-TP and/or TEO slightly induced the porosity and roughness of the films as compared to film N0. It could be attributed to the migration of oil to the film surface during air drying (Dammak et al., 2017; Tessaro et al., 2021). Similar phenomenon was also observed in gelatin/chitosan-based films with non-emulsified essential oils (Bonilla et al., 2018). Besides, the intact bio-composite films indicated the even distribution of the nanoemulsified active compounds for their excellent compatibility within the film matrix, which agreed well with the observation in CLSM images (Fig. 1C). These results suggested that FG/CS-based films could be confidently applied for delivery of active compounds such as α-TP and TEO for food preservation.

3.3. Metabolic changes of chill-stored golden pomfret fillets under different treatments

NMR-based metabolomics strategy was performed to elucidate the mechanism of active packaging on fish preservation during refrigerated storage. The representative ^{1}H NMR spectra of golden pomfret fillets packed with various active films during chilled storage are shown in Figs. 2A and S3 (Supplementary Material). In total, forty-seven metabolites were explicitly identified based on the 2D NMR analysis (^{1}H–^{13}C HSQC) and metabolic databases (Fig. 2B and Table S1 in Supplementary Material), which could be grouped into amino acids, organic acids, carbohydrates, alcohols, biogenic amines, nucleotides, and other metabolites.

To deeply understand the metabolic changes in stored golden pomfret fillets under different treatments, PCA was carried out to illustrate the discrepancies of metabolite variations within different treatment groups. As shown in Fig. 3A, the high values of R^2X (0.939) and Q^2 (0.879) imparted excellent interpretation and prediction capability to the PCA model. In the 3D score plot (Fig. 3B), different treatment groups exhibited distinct separations, among which the fresh fillet group (day 0, I) was recognizably separated from its counterparts (II, III, IV, and V) on day 12. Moreover, the treated groups (III and IV) were well clustered in each group and were clearly separated from their combination (V). These observations confirmed the fish fillets' discriminative metabolic responses to quality deterioration during chilled storage when employed with different biopreservatives for preservation.

Moreover, the dominating metabolites responsible for the group separation are depicted in the loading plot (Fig. 3C). For example, metabolites such as 2,3-butanediol, creatine, tyrosine, aspartic acid, valine, alanine, and glycine dominated in PC1, while those such as ethanol, threonine, anserine, and maltose featured in PC2. These metabolites may serve as potential biomarkers for fish spoilage during chilled storage.

Furthermore, pairwise comparisons were conducted by OPLS-DA to investigate the metabolic changes in chill-stored golden pomfret fillets with various active packaging. Specifically, the identified metabolites from the fresh fillets (day 0, I) were compared with those from treatment groups on day 12 (II, III, IV, and V), respectively. Besides, pairwise comparisons between groups III/IV and V were carried out to determine the metabolic disparities in stored fish fillets treated with individual biopreservative and their combinations. The results were exhibited as cross-validated score plots and corresponding coefficient plots. The R^2X and Q^2 were 0.969 and 1 for paired I-II, 0.881 and 0.993 for paired I-III, 0.835 and 0.988 for paired I-IV, 0.941 and 0.997 for paired I-V, 0.958 and 0.997 for paired III-V, and 0.909 and 0.993 for paired IV-V, respectively. The high values of R^2X and Q^2 indicated the high quality of the OPLS-DA model with good fitness and predictability (He et al., 2021). As shown in Fig. 4(A1-F1), each paired group was distinctly separated, demonstrating that the metabolic variations in chill-stored golden pomfret fillets with various biopreservatives could be differentiated. The coefficient plots (Fig. 4(A2-F2)) were also applied to screen the marked metabolites that were largely responsible for the pairwise differentiation, among which metabolites located in the negative and positive side of coefficient axis indicated the lower and higher relative concentrations, respectively between the paired groups (Lin et al., 2022). The metabolites with VIP >1 in each paired group were considered greatly affected by different treatments during storage (Zhao, et al., 2019). Compared to the fresh fillets (day 0, I), a total of 39 metabolites were found to be markedly influenced by the FG/CS-based films, among which 17 metabolites such as tyramine, methylamine, hypoxanthine, lactic acid, acetic acid, and 3-hydroxybutyric acid increased in the group II after 12 days, whereas the rest including choline, betaine, glycine, and glycogen decreased during the refrigerated storage. The accumulation of organic acids such as lactic acid and acetic acid indicated the anaerobic glycolysis of glycogen in fish muscle for supplying energy during storage (Choe et al., 2008; Scheffler &

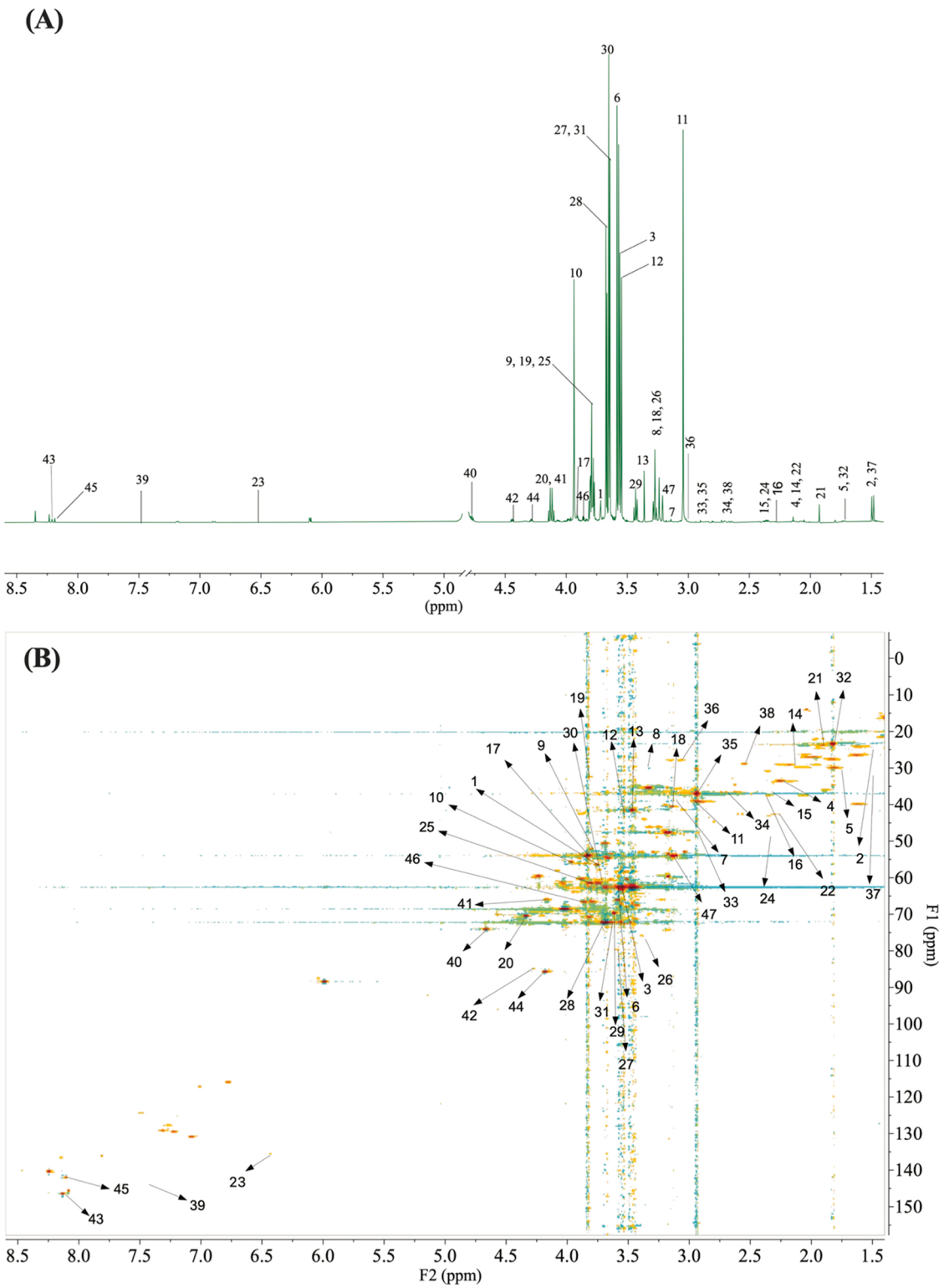

Fig. 2. Representative 1D ^{1}H NMR spectra (A) and 2D ^{1}H–^{13}C NMR spectra (B) of chill-stored golden pomfret fillets. Note: 1. Leu; 2. Ile; 3. Val; 4. Met; 5. Lys; 6. Thr; 7. Phe; 8. His; 9. Ala; 10. Tyr; 11. Cre; 12. Gly; 13. Tau; 14. Gln; 15. Glu; 16. GABA; 17. Asp; 18. Arg; 19. Anserine; 20. Lactic acid; 21. Acetic acid; 22. Butyric acid; 23. Fumaric acid; 24. 3-Hydroxybutyric acid; 25. α-glucose; 26. β-glucose; 27. Glycogen; 28. Maltose; 29. Sucrose; 30. Ethanol; 31. 2,3-Butanediol; 32. Putrescine; 33. TMA; 34. DMA; 35. Tyramine; 36. Histamine; 37. Cadaverine; 38. Methylamine; 39. Uracil; 40. ATP; 41. ADP; 42. AMP; 43. IMP; 44. HxR; 45. Hx; 46. Betaine; 47. Choline.

Gerrard, 2007). The production of biogenic amines such as putrescine, histamine, and tyramine reflected the fish spoilage during storage (Prabhakar et al., 2020), resulting from the decarboxylation of lysine, histidine, and tyrosine, respectively (Jinadasa et al., 2016; Romero-González et al., 2012). Although the fish spoilage is a natural process caused by the digestive enzymes, surface bacteria, as well as lipid oxidation (Prabhakar et al., 2020), the presence of α-TP or TEO in the FG/CS-based films inhibited the breakdown of certain amino acids

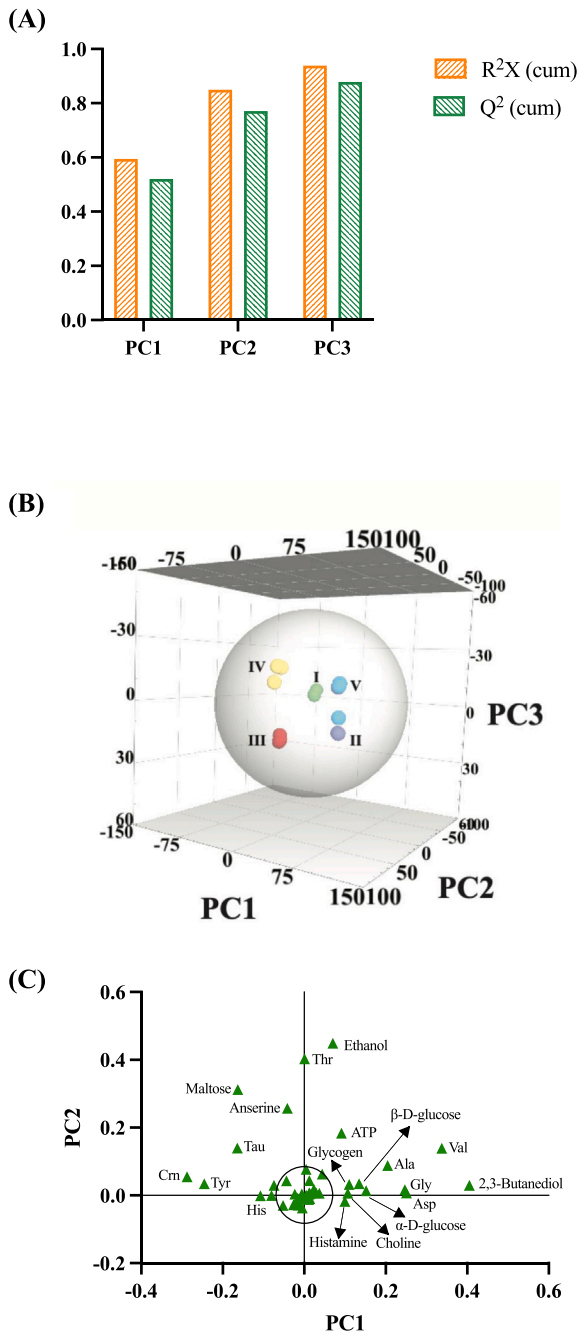

Fig. 3. Principal component analysis (PCA) of ^{1}H NMR spectra for the metabolite profiles of golden pomfret extracts. The variances are explained by principal components in PCA (A); the 3D score plot of PCA (B); and the loading plot of PCA (C). Note: I, fresh golden pomfret fillets on day 0; II, III, IV and V represents chill-stored golden pomfret fillets on day 12 under different bioploymer films wrapping (N1-N4), respectively. (N1) Fish gelatin/chitosan-based (FG/CS-based) films loaded with nanoemulsions (without active compounds); (N2) FG/CS-based films loaded with nanoemulsified α-tocopherol; (N3) FG/CS-based films loaded with nanoemulsified thyme essential oil; (N4) FG/CS-based films loaded with nanoemulsified α-tocopherol and thyme essential oil.

and formation of their degraded compounds such as cadaverine and tyramine (Fig. 4(B2-D2)). Notably, as shown in Fig. 4(E2 & F2), combination of α-TP and TEO led to decreased levels of biogenic amines including TMA, DMA, histamine, and cadaverine as compared to their individual application in fish preservation, whereas certain carbohydrates (sucrose and maltose) and amino acids (creatine, arginine, tyrosine, and histidine) were maintained at higher relative levels. Their combination also hampered the degradation of inosine and accumulation of hypoxanthine within the storage time due to nucleotide breakdown, mainly resulting from autolysis of endogenous enzymes along with bacteria spoilage (Li et al., 2017), which may contribute to the desirable textural quality. These together help maintain the suitable physicochemical and sensory characteristics of fish muscle. The results may indicate the potential application of FG/CS-based films loaded with nanoemulsified α-TP and TEO as active packaging for fish preservation.

3.4. Pathway analysis

The underlying mechanisms of preservative effects of α-TP and TEO on fish muscle during refrigerated storage were revealed based on the disturbed metabolic pathways that were identified through the screened principal metabolites. Volcano plots shown in Fig. 5 were based on the correlation coefficients, P values, and fold changes (FCs) and the pathway analysis was carried out based on the screened metabolites. Those with P value < 0.05 and FCs > 2.0 (or FCs < 0.5) were of significant statistics (Zhao et al., 2020). It is worth noticing that the altered metabolites among different treatment groups were primarily distributed in the top right region of the volcano plots (Fig. 5(A1-D1)), indicating that the individual treatment mainly led to accumulated metabolite contents in the golden pomfret fillets during chilled storage. For example, a total of 30 metabolites showed marked alterations ($P < 0.05$) (Fig. 5(A1)), among which 18 metabolites including some carbohydrates (glucose, maltose, and glycogen), amino acids (valine, alanine, glycine, and aspartate) and alcohols (ethanol and 2,3-butanediol) located in the right side of the volcano plot were marked with orange points, representing the growth of these metabolites in the chill-stored fish fillets as compared to the fresh fish fillets. The increased trends in amino acids could be attributed to the protein hydrolysis induced by bacterial spoilage (Moczkowska et al., 2017). However, the presence of α-TP and TEO protected the fish muscle from quality deterioration during storage by inhibiting the glycolysis and degradation of adenine nucleotides, confirmed with the reduction of organic acids and biogenic amines (Fig. 5(B1-D1)). Notably, combination of α-TP and TEO led to the optimal preservative effects on fish muscle by inhibiting the production of some typical spoilage inducing substances such as tyramine and methylamine.

Furthermore, pathway analysis was conducted to identify the metabolic pathways within different treatment groups based on the screened metabolites and database (Fig. 5(A2-F2) and Table S2 in Supplementary Material). As shown in Fig. 5(A2), the total of 33 pathways were predicted and 11 of them were considered significant pathways in the group II on day 12. The disturbed pathways were aminoacyl-tRNA biosynthesis; histidine metabolism; valine, leucine, and isoleucine biosynthesis; glycolysis/gluconeogenesis; phenylalanine, tyrosine, and tryptophan biosynthesis; glycine, serine, and threonine metabolism; beta-alanine metabolism; phenylalanine metabolism; alanine, aspartate, and glutamate metabolism; glyoxylate and dicarboxylate metabolism; and arginine biosynthesis. The identified interfered pathways were mainly related with amino acid biosynthesis and carbohydrate metabolism. However, two more pathways, namely, purine metabolism and glutathione metabolism were identified as significant pathways for the chill-stored fish fillets treated with nanoemulsified TEO (Fig. 5(C2)). As for fish fillets treated with combination of α-TP and TEO, twelve significant pathways were altered, the number of which reflected the synergistic effects of α-TP and TEO on fish preservation (Fig. 5(D2)). Moreover, the combined treatment of α-TP and TEO significantly changed 11 and 8 metabolic pathways as compared to its individual component (Fig. 5(E2 & F2)), respectively, which further confirmed the stronger preservative effects of the FG/CS-based films loaded with nanoemulsified α-TP and TEO on fish muscle than their counterparts.

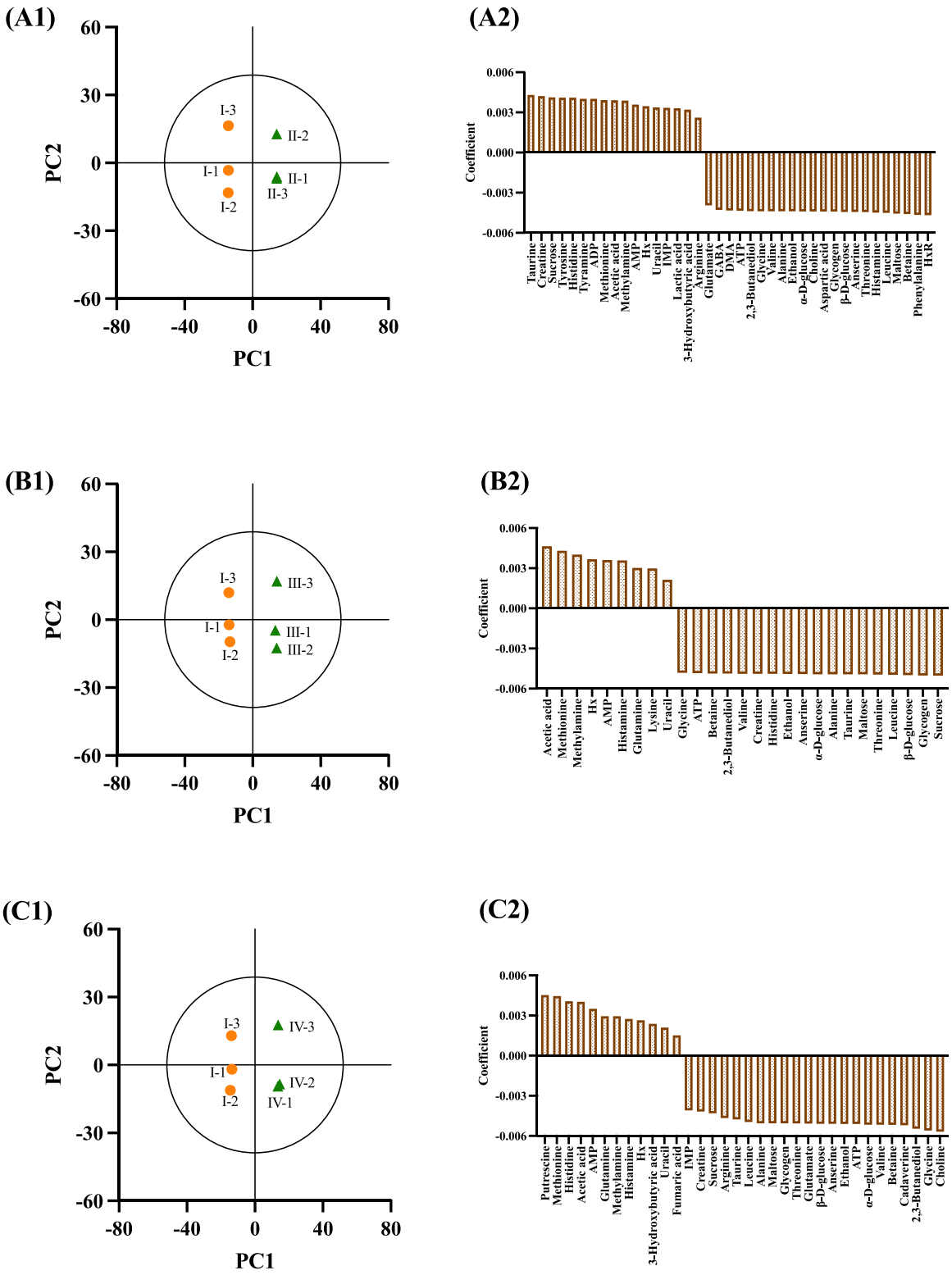

Fig. 4. Orthogonal projection to latent structures-discriminant analysis (OPLS-DA) of the metabolic profiles of golden pomfret fillets under different treatments during storage. Note: I, fresh golden pomfret fillets on day 0; II, III, IV and V represents stored golden pomfret fillets on day 12 under different bioploymer films wrapping (N1-N4), respectively. (N1) Fish gelatin/chitosan-based (FG/CS-based) films loaded with nanoemulsions (without active compounds); (N2) FG/CS-based films loaded with nanoemulsified α-tocopherol; (N3) FG/CS-based films loaded with nanoemulsified thyme essential oil; (N4) FG/CS-based films loaded with nanoemulsified α-tocopherol and thyme essential oil.

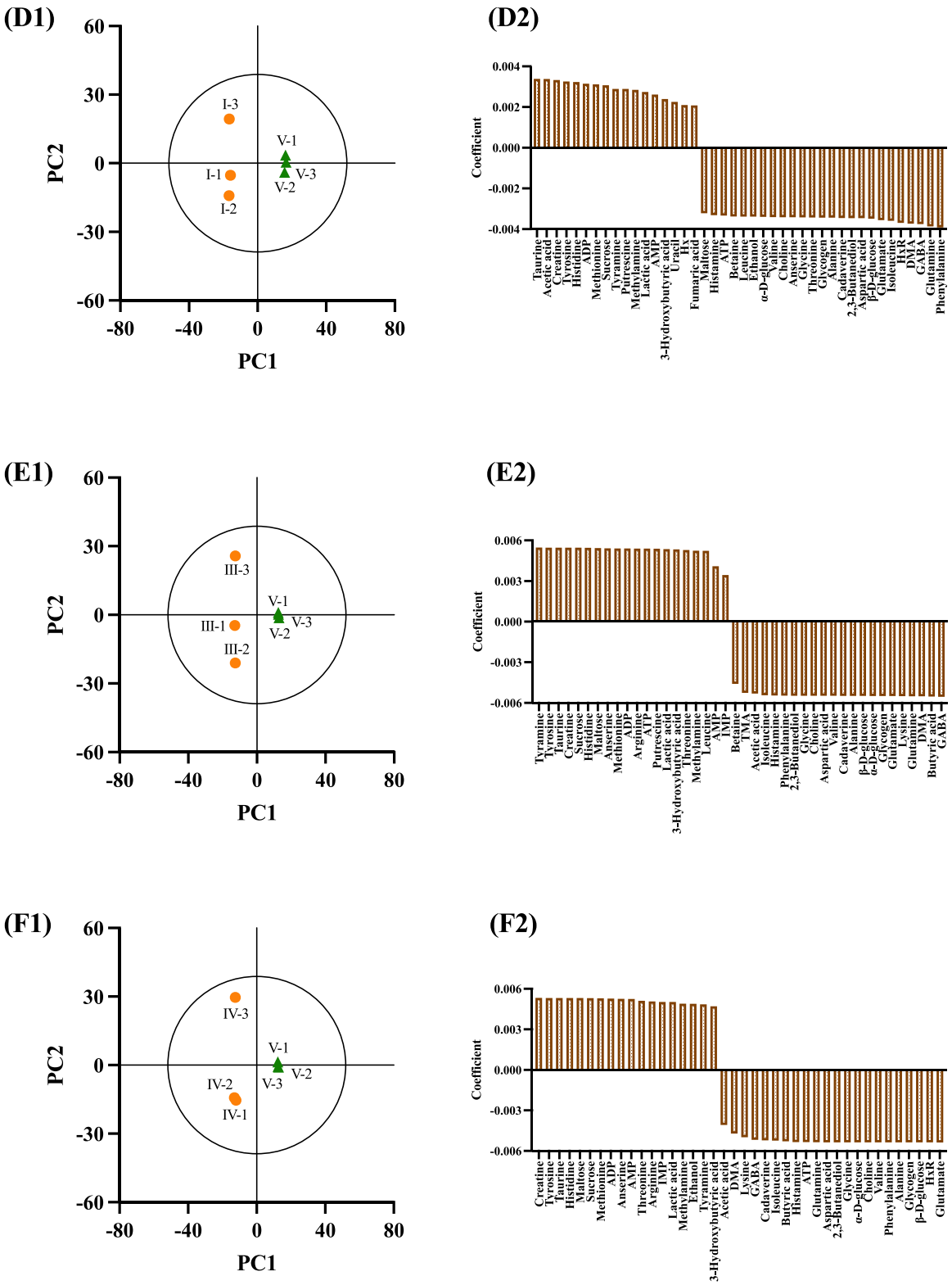

Fig. 4. (*continued*).

3.5. Metabolic alterations of chill-stored golden pomfret fillets under different treatments

The metabolic changes in golden pomfret fillets treated with various active films during chilled storage are summarized in Fig. 6 based on the KEGG metabolic pathway analysis. Color transformation from purple to orange indicated the gradual increase in metabolite concentrations extracted from different treatment groups (I-V). Four major metabolic pathways were proposed, namely amino acid metabolism, carbohydrate metabolism, nitrogen metabolism, and nucleotide metabolism, among which amino acid metabolism was the most affected pathway under different treatments. Both increasing and decreasing trends in amino acid concentrations were observed in the chill-stored golden pomfret fillets. For instance, the higher levels of amino acids (e.g., valine,

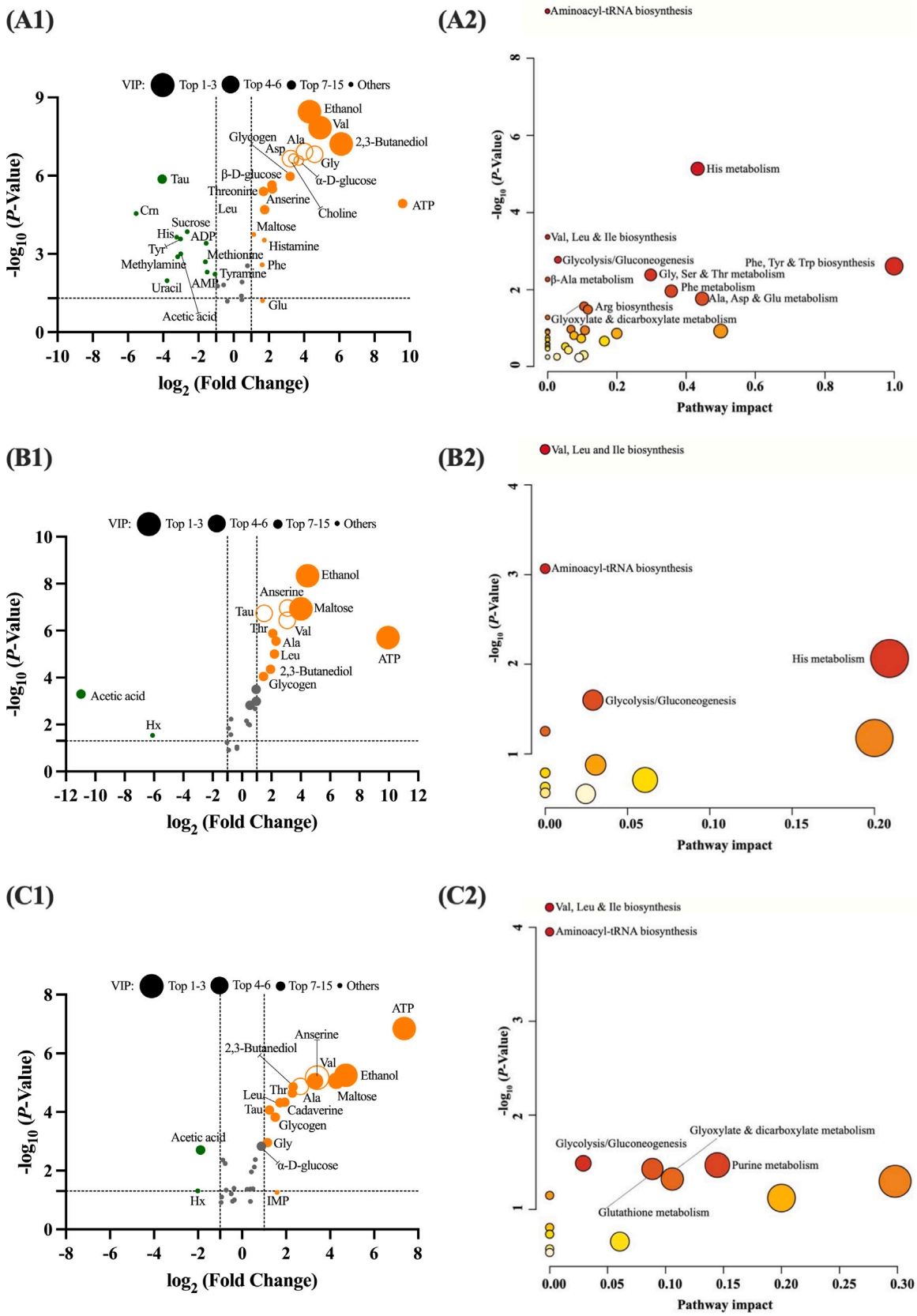

Fig. 5. Volcano plots (A1-F1) and pathway analysis (A2-F2) for comparing the metabolic profiles of golden pomfret fillets under different treatments during storage. Note: the volcano plots exhibit the crucial metabolites ($P < 0.05$ and FCs > 2.0 or FCs < 0.5). Green colour represents decreased metabolite amounts while orange colour represents increased metabolite amounts during storage. I, fresh golden pomfret fillets on day 0; II, III, IV and V represents stored golden pomfret fillets on day 12 under different bioploymer films wrapping (N1-N4), respectively. (N1) Fish gelatin/chitosan-based (FG/CS-based) films loaded with nanoemulsions (without active compounds); (N2) FG/CS-based films loaded with nanoemulsified α-tocopherol; (N3) FG/CS-based films loaded with nanoemulsified thyme essential oil; (N4) FG/CS-based films loaded with nanoemulsified α-tocopherol and thyme essential oil.

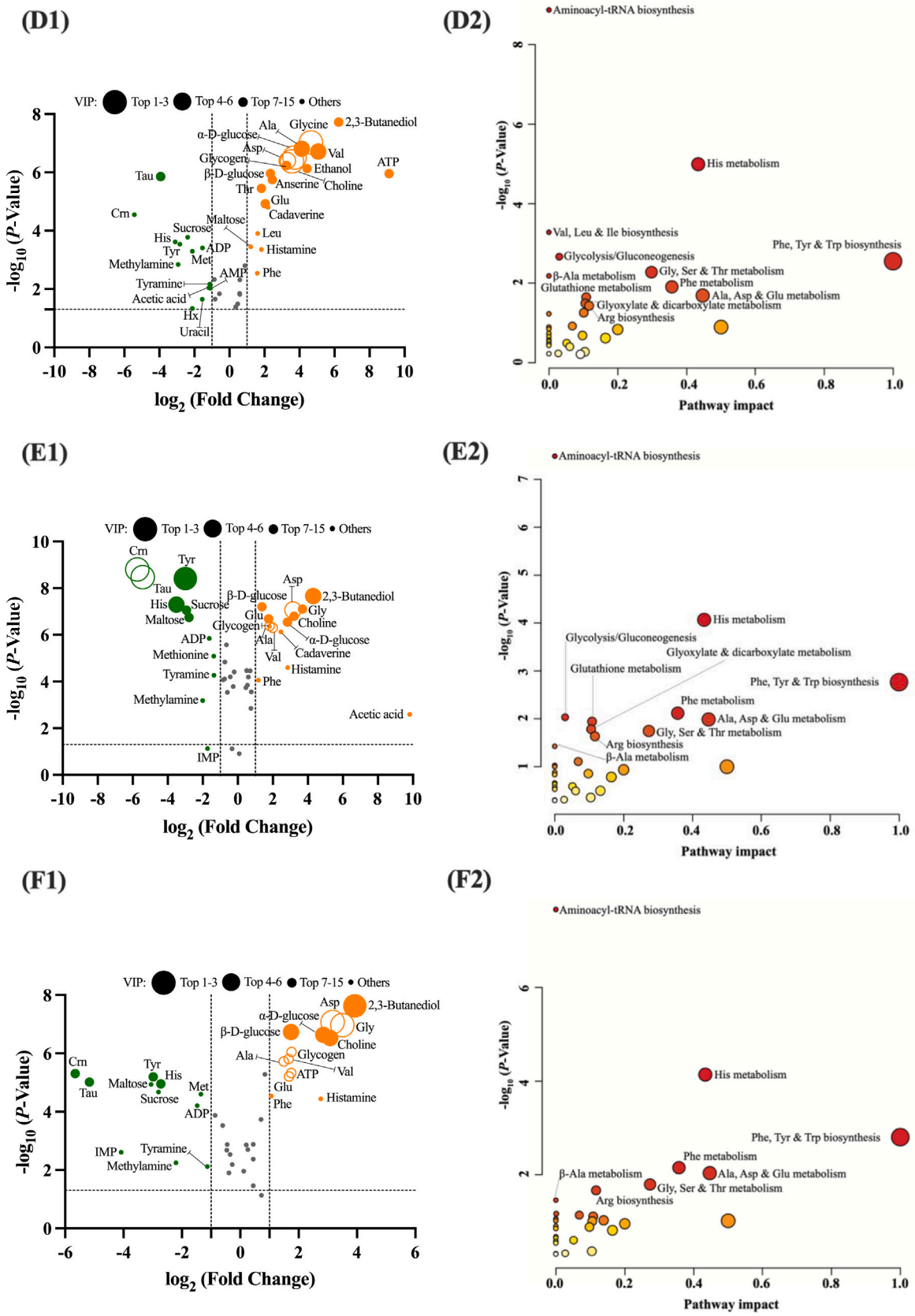

Fig. 5. (*continued*).

glycine, alanine, glutamate, aspartate, and anserine) may result from protein hydrolysis by the extracellular proteases of spoilage microorganisms (Hai et al., 2022; Lou et al., 2021), whereas the lower levels of amino acids such as methionine, creatine, tyrosine, and lysine were observed in comparison of the group I. The presence of α-TP and TEO inhibited the biosynthesis of some amino acids such as valine, glycine,

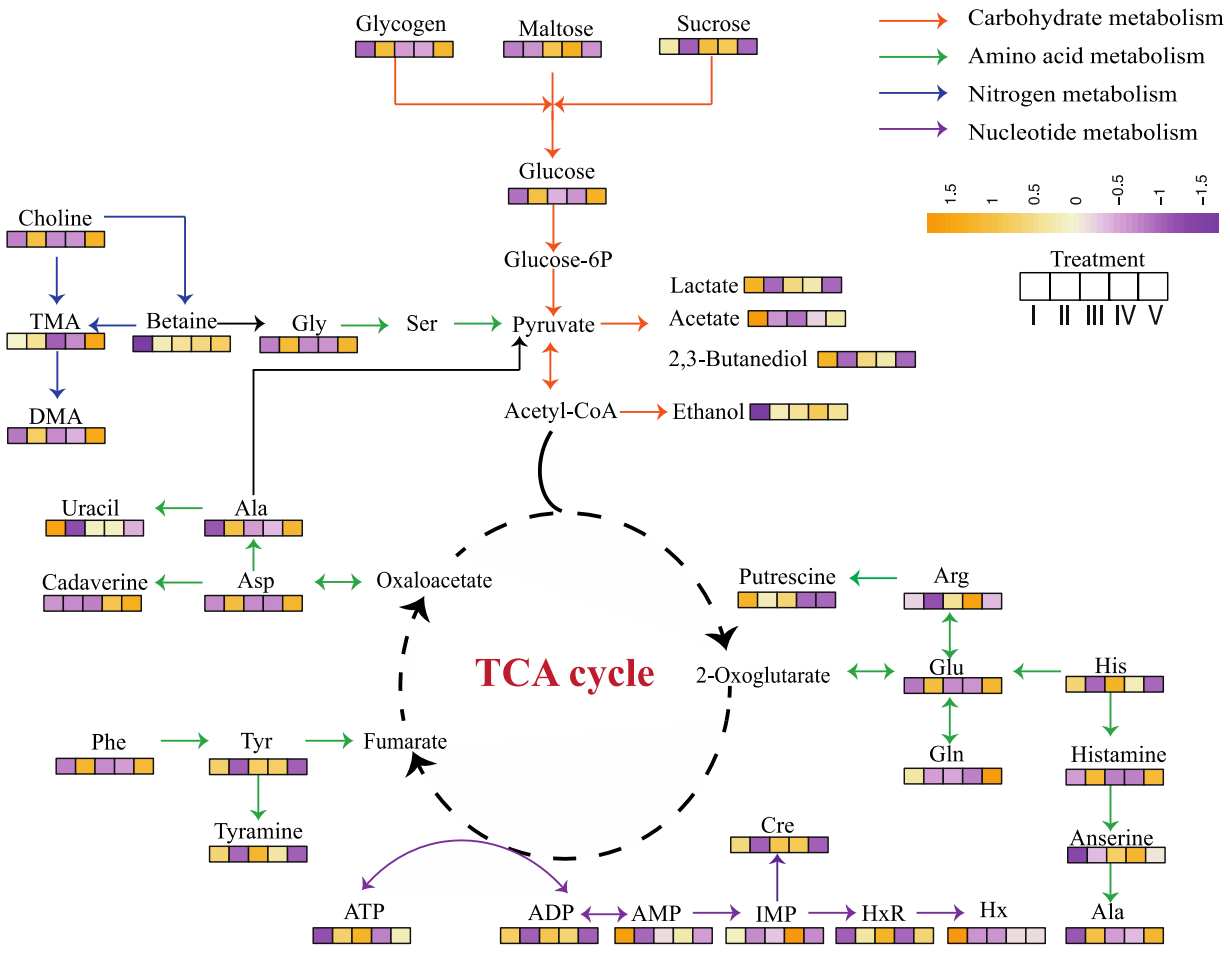

Fig. 6. The alterations of marked metabolites in golden pomfret fillets under different treatments during storage. Note: I, fresh golden pomfret fillets on day 0; II, III, IV and V represents stored golden pomfret fillets on day 12 under different bioploymer films wrapping (N1-N4), respectively. (N1) Fish gelatin/chitosan-based (FG/CS-based) films loaded with nanoemulsions (without active compounds); (N2) FG/CS-based loaded with nanoemulsified α-tocopherol; (N3) FG/CS-based films loaded with nanoemulsified thyme essential oil; (N4) FG/CS-based films loaded with nanoemulsified α-tocopherol and thyme essential oil.

and glutamate that function as osmoprotectants to protect cellular constituents. The downregulated biosynthesis of these amino acids may perturb the equilibrium of cytoplasmic osmolality, which further disintegrates the cellular structure (Baptista et al., 2020; Hai et al., 2022; Zhao et al., 2020). The decreased levels of those amino acids, such as arginine and aspartate serving as alternative carbon sources revealed that the preservative activities may also be raised through disturbing the TCA cycle from providing metabolism energy for bacteria growth (Hai et al., 2022).

Biogenic amines can work as efficient biochemical indicators of fish quality and freshness. The typical spoilage inducing substances including TMA, DMA, cadaverine, tyramine, histamine, and putrescine were identified in our study. The formation of TMA can occur during fish storage through TMAO degradation and breakdown of certain substances including choline and betaine, which are mainly responsible for the fishy odor (Prabhakar et al., 2020). The decarboxylation of amino acids such as tyrosine, histidine, and lysine can produce their toxic derivatives, i.e., tyramine, histamine, and putrescine, respectively (Yongsawatdigul et al., 2004). Although putrescine causes indirect toxicity to the fishes, its appearance together with cadaverine can drive the histamine allergy (Prabhakar et al., 2020). As shown in Fig. 6, the biogenic amines generally exhibited an increasing trend in the chill-stored fish fillets, but to different extents with different treatments. Combination of α-TP and TEO lessened the production of tyramine and putrescine, while the amount of cadaverine in all treated samples increased during chilled storage. The fish freshness may be maintained through interrupting the nitrogen metabolism of microorganisms, reducing the production of biogenic amines via decarboxylation of amino acids (Jasour et al., 2018).

Sugars such as glycogen, maltose, sucrose, and glucose were the major carbohydrates in the golden pomfret fillets, which could provide carbon sources entering the TCA cycle to generate energy for spoilage bacteria. Production of organic acids like lactate and acetate, along with alcohols such as ethanol and 2,3-butanediol resulted from microbial growth in fish muscle (Prabhakar et al., 2020). In our study, the relative higher concentrations of sugars like glycogen and glucose in treated fish muscle may indicate the inhibition of sugar degradation by hydrolysis and glycolysis (Zhao et al., 2020). Furthermore, the relative lower concentrations of alcohols like ethanol and 2,3-butanediol in treated fish muscle implied that the active packaging reduced the production of such unfavorable odor and maintained fish freshness during refrigerated storage.

Nucleotide metabolism was also found in golden pomfret fillets during chilled storage, which is the process of the autolytic decomposition of ATP and formation of its by-products including ADP, AMP, IMP, HxR, and Hx (Prabhakar et al., 2020). The production of HxR and Hx contributes to off-flavors in fish muscle and is associated with deterioration of fish quality (Zhao et al., 2020). In our study, fish fillets treated with nanoemulsified TEO had the highest level of IMP that could provide fish with umami flavor. Meanwhile, the contents of HxR and Hx were maintained at relative lower level, indicating that nanoemulsified TEO actively mediated the nucleotide metabolism of chill-stored fish fillets,

thanks to its inhibitory effects on microbial growth (Huang et al., 2018).

3.6. Quality changes in chill-stored golden pomfret fillets under different treatments

TVB-N is a major parameter to measure the volatile nitrogenous bases present in fish, which gives an accurate estimation of fish freshness (Ricque-Marie et al., 1998). Therefore, it is employed to better understand the effect of the active packaging on the fish quality and freshness during storage. As shown in Fig. 7, the TVB-N value in our study showed an increasing trend for all fish samples during the 15-day storage, mainly resulting from the summation of ammonia and amine produced by spoilage bacteria and endogenous enzymes (Prabhakar et al., 2020). After 6-day storage, the TVB-N value of control 0 (fish fillets without treatment) sharply increased from the initial value of 2.8 mg/100 g to over 30 mg/100 g, which is the upper limit of TVB-N value for golden pomfret (Lou et al., 2021). Fish fillets treated with FG/CS-based films without active compounds loaded extended the shelf life of fish muscle to 9 days during chilled storage, while there was no significant difference of TVB-N value between the two treatment groups (control 1 and control 2). Interestingly, α-TP exhibited a stronger inhibitory effect on fish deterioration than its counterparts during 9-day storage, whereas combination of α-TP and TEO overtook α-TP as the optimal preservative for fish quality in the following 6-day storage. These results suggested that FG/CS-based films loaded with α-TP and TEO could effectively restrain the accumulation of TVB-N in chill-stored fish muscle and extend its shelf life.

3.7. Schematic illustration

Based on the previous results, a potential schematic of the effect of FG/CS-based active films on the metabolic profiles and fish quality and freshness of golden pomfret fillets during chilled storage was proposed as shown in Fig. 8. The biodegradable active films maintained the nutritional value and prolonged the shelf-life of fish fillets during chilled storage through inhibiting the bacteria spoilage and fish protein degradation, which could be indicated by the rapid decrease in TVB-N value. Moreover, the intrinsic antimicrobial property of chitosan coupled with the incorporation of functional ingredients (α-TP and/or TEO) imparted a protectant effect on the golden pomfret fillets during chilled storage, mainly with four metabolic pathways involved. For example, the production of biogenic amines including histamine, putrescine, and cadaverine was restrained during storage through inhibition of protein hydrolysis to amino acids that can be further transformed to biogenic amines (Zhao et al., 2019). The hydrolysis and glycolysis of sugars were also retarded by active packaging and their major derivatives were organic acids and alcohols that are responsible for fish off-odors. Besides, the transformation of nucleotides to inosine and hypoxanthine was intervened by active packaging through inactivation of endogenous enzymes and microorganisms (Zhao et al., 2019).

Overall, the protectant effect of the active packaging on chill-stored golden pomfret fillets could be summarized that inclusion of biopreservatives along with chitosan collectively retarded fish spoilage during chilled storage via intervening the metabolic pathways of chill-stored fish fillets including amino acid metabolism, carbohydrate metabolism, nitrogen metabolism, and nucleotide metabolism. These inhibitors together endowed the FG/CS-based active films with inhibitory effects on the spoilage of golden pomfret fillets during refrigerated storage.

4. Conclusion

In our study, biodegradable fish gelatin/chitosan-based active films incorporated with nanoemulsified α-tocopherol and thyme essential oil were successfully developed using casting technique. These active films possessed a homogenous surface structure with the nanoemulsified bioactive materials evenly distributed within their matrix. Incorporation of α-TP sharply reduced the water solubility of the films. Besides, inclusion of α-TP and TEO synergistically improved the preservative effects of the films on golden pomfret fillets during chilled storage. Furthermore, metabolic changes in stored fish fillets under different treatments were revealed through NMR analysis. Four major metabolic pathways were identified, namely amino acid, carbohydrate, nitrogen, and nucleotide metabolism. Combination of α-TP and TEO provided desirable inhibitory effects on the formation of unfavourable compounds that may exert off-odours and facilitate the deterioration of fish quality during storage. These results suggest that the biodegradable fish gelatin/chitosan-based films could be used as efficient vehicles for delivery of bioactive compounds for preservation and shelf-life extension of foodstuffs.

CRediT authorship contribution statement

Yi Liu: Conceptualization, Methodology, Investigation, Formal analysis, Writing – original draft, Writing – review & editing. **Yi Kai:** Methodology, Investigation. **Hongshun Yang:** Conceptualization, Supervision, Funding acquisition, Writing – review & editing.

Declaration of Competing Interest

The authors declare that they have no known competing financial interests or personal relationships that could have appeared to influence the work reported in this paper.

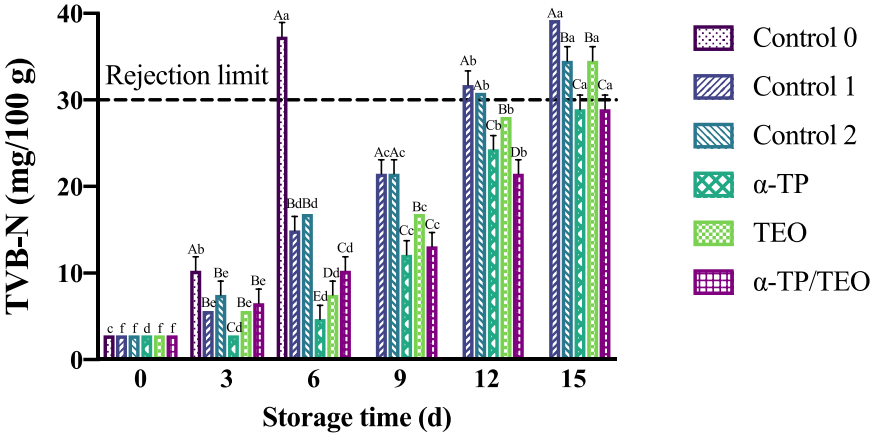

Fig. 7. TVB-N values of chill-stored golden pomfret fillets under different treatments. Bars represent standard deviation (n = 3). Means within each storage time with different uppercase letters are significantly different among different treatments ($P < 0.05$); Means within each group with different lowercase letters are significantly different among different storage time ($P < 0.05$). Note: Control 0: fillets with no treatment; Control 1: fillets treated with FG/CS-based films (without nanoemulsions); Control 2: fillets treated with FG/CS-based films loaded with nanoemulsions (without active compounds); α-TP: fillets treated with FG/CS-based films loaded with nanoemulsified α-tocopherol; TEO: fillets treated with FG/CS-based films loaded with nanoemulsified thyme essential oil; α-TP/TEO: fillets treated with FG/CS-based films loaded with nanoemulsified α-tocopherol and thyme essential oil.

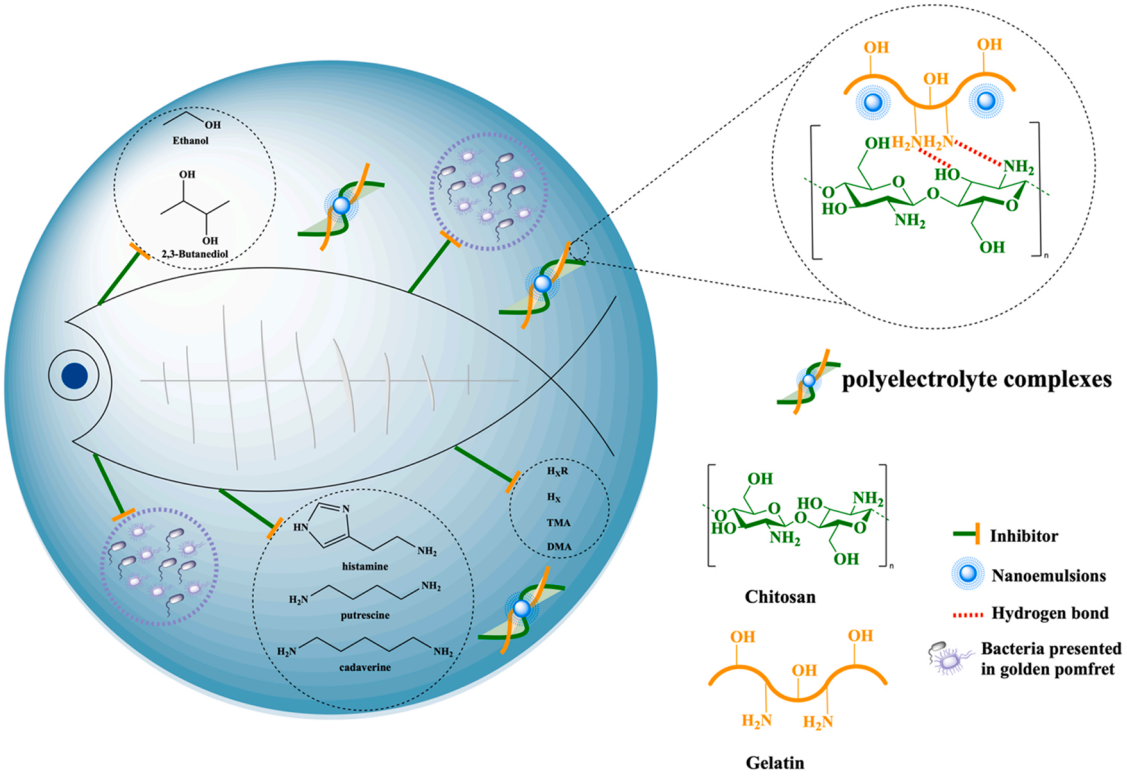

Fig. 8. Proposed schematic of the effect of FG/CS-based active films on the metabolic profiles and fish quality and freshness of golden pomfret fillets during chilled storage.

Data availability

Data will be made available on request.

Acknowledgements

This study was financially supported by Singapore Ministry of Education Academic Research Fund Tier 1 (A-8000469–00-00).

Appendix A. Supporting information

Supplementary data associated with this article can be found in the online version at doi:10.1016/j.fpsl.2023.101046.

References

Bahrami, A., Delshadi, R., Assadpour, E., Jafari, S. M., & Williams, L. (2020). Antimicrobial-loaded nanocarriers for food packaging applications. *Advances in Colloid and Interface Science, 278*, Article 102140. https://doi.org/10.1016/j.cis.2020.102140

Baptista, R. C., Horita, C. N., & Sant'Ana, A. S. (2020). Natural products with preservative properties for enhancing the microbiological safety and extending the shelf-life of seafood: A review. *Food Research International, 127*, Article 108762. https://doi.org/10.1016/j.foodres.2019.108762

Benbettaïeb, N., Karbowiak, T., Brachais, C.-H., & Debeaufort, F. (2015). Coupling tyrosol, quercetin or ferulic acid and electron beam irradiation to cross-link chitosan-gelatin films: A structure-function approach. *European Polymer Journal, 67*, 113–127. https://doi.org/10.1016/j.eurpolymj.2015.03.060

Bhowmik, S., Agyei, D., & Ali, A. (2022). Bioactive chitosan and essential oils in sustainable active food packaging: Recent trends, mechanisms, and applications. *Food Packaging and Shelf Life, 34*, Article 100962. https://doi.org/10.1016/j.fpsl.2022.100962

Bonilla, J., Poloni, T., Lourenço, R. V., & Sobral, P. J. A. (2018). Antioxidant potential of eugenol and ginger essential oils with gelatin/chitosan films. *Food Bioscience, 23*, 107–114. https://doi.org/10.1016/j.fbio.2018.03.007

Cen, S., Fang, Q., Tong, L., Yang, W., Zhang, J., Lou, Q., & Huang, T. (2021). Effects of chitosan-sodium alginate-nisin preservatives on the quality and spoilage microbiota of *Penaeus vannamei* shrimp during cold storage. *International Journal of Food Microbiology, 349*, Article 109227. https://doi.org/10.1016/j.ijfoodmicro.2021.109227

Chang, Y., McLandsborough, L., & McClements, D. J. (2012). Physical properties and antimicrobial efficacy of thyme oil nanoemulsions: Influence of ripening inhibitors. *Journal of Agricultural and Food Chemistry, 60*(48), 12056–12063. https://doi.org/10.1021/jf304045a

Chen, H., Hu, X., Chen, E., Wu, S., McClements, D. J., Liu, S., Li, B., & Li, Y. (2016). Preparation, characterization, and properties of chitosan films with cinnamaldehyde nanoemulsions. *Food Hydrocolloids, 61*, 662–671. https://doi.org/10.1016/j.foodhyd.2016.06.034

Choe, J. H., Choi, Y. M., Lee, S. H., Shin, H. G., Ryu, Y. C., Hong, K. C., & Kim, B. C. (2008). The relation between glycogen, lactate content and muscle fiber type composition, and their influence on postmortem glycolytic rate and pork quality. *Meat Science, 80*(2), 355–362. https://doi.org/10.1016/j.meatsci.2007.12.019

Dammak, I., Bittante, A. M. Q. B., Lourenço, R. V., & do Amaral Sobral, P. J. (2017). Properties of gelatin-based films incorporated with chitosan-coated microparticles charged with rutin. *International Journal of Biological Macromolecules, 101*, 643–652. https://doi.org/10.1016/j.ijbiomac.2017.03.163

Gómez-Estaca, J., López de Lacey, A., López-Caballero, M. E., Gómez-Guillén, M. C., & Montero, P. (2010). Biodegradable gelatin-chitosan films incorporated with essential oils as antimicrobial agents for fish preservation. *Food Microbiology, 27*(7), 889–-896. https://doi.org/10.1016/j.fm.2010.05.012

Gulzar, S., Tagrida, M., Prodpran, T., & Benjakul, S. (2022). Antimicrobial film based on polylactic acid coated with gelatin/chitosan nanofibers containing nisin extends the shelf life of Asian seabass slices. *Food Packaging and Shelf Life, 34*, Article 100941. https://doi.org/10.1016/j.fpsl.2022.100941

Haghighi, H., De Leo, R., Bedin, E., Pfeifer, F., Siesler, H. W., & Pulvirenti, A. (2019). Comparative analysis of blend and bilayer films based on chitosan and gelatin enriched with LAE (lauroyl arginate ethyl) with antimicrobial activity for food packaging applications. *Food Packaging and Shelf Life, 19*, 31–39. https://doi.org/10.1016/j.fpsl.2018.11.015

Hai, Y., Zhou, D., Lam, Y. L. N., Li, X., Chen, G., Bi, J., Lou, X., Chen, L., & Yang, H. (2022). Nanoemulsified clove essential oils-based edible coating controls *Pseudomonas* spp.-causing spoilage of tilapia (*Oreochromis niloticus*) fillets: Working mechanism and bacteria metabolic responses. *Food Research International, 159*, Article 111594. https://doi.org/10.1016/j.foodres.2022.111594

He, Y., Zhao, X., Chen, L., Zhao, L., & Yang, H. (2021). Effect of electrolysed water generated by sodium chloride combined with sodium bicarbonate solution against *Listeria innocua* in broth and on shrimp. *Food Control, 127*, Article 108134. https://doi.org/10.1016/j.foodcont.2021.108134

Huang, Z., Liu, X., Jia, S., Zhang, L., & Luo, Y. (2018). The effect of essential oils on microbial composition and quality of grass carp (*Ctenopharyngodon idellus*) fillets during chilled storage. *International Journal of Food Microbiology, 266*, 52–59. https://doi.org/10.1016/j.ijfoodmicro.2017.11.003

Jasour, M. S., Wagner, L., Sundekilde, U. K., Larsen, B. K., Rasmussen, H. T., Hjermitslev, N. H., Hammershøj, M., Dalsgaard, A. J. T., & Dalsgaard, T. K. (2018). Fishmeal with different levels of biogenic amines in aquafeed: Comparison of feed

protein quality, fish growth performance, and metabolism. *Aquaculture, 488*, 80–89. https://doi.org/10.1016/j.aquaculture.2018.01.030

Jégou, C., Kervarec, N., Cérantola, S., Bihannic, I., & Stiger-Pouvreau, V. (2015). NMR use to quantify phlorotannins: The case of *Cystoseira tamariscifolia*, a phloroglucinol-producing brown macroalga in Brittany (France). *Talanta, 135*, 1–6. https://doi.org/10.1016/j.talanta.2014.11.059

Jinadasa, B. K. K. K., Jayasinghe, G. D. T. M., & Ahmad, S. B. N. (2016). Validation of high-performance liquid chromatography (HPLC) method for quantitative analysis of histamine in fish and fishery products. *Cogent Chemistry, 2*(1), 1156806. https://doi.org/10.1080/23312009.2016.1156806

Kakaei, S., & Shahbazi, Y. (2016). Effect of chitosan-gelatin film incorporated with ethanolic red grape seed extract and *Ziziphora clinopodioides* essential oil on survival of *Listeria monocytogenes* and chemical, microbial and sensory properties of minced trout fillet. *LWT - Food Science and Technology, 72*, 432–438. https://doi.org/10.1016/j.lwt.2016.05.021

Kanatt, S. R., Rao, M., Chawla, S., & Sharma, A. (2012). Active chitosan-polyvinyl alcohol films with natural extracts. *Food Hydrocolloids, 29*(2), 290–297. https://doi.org/10.1016/j.foodhyd.2012.03.005

Kumar, S., Shukla, A., Baul, P. P., Mitra, A., & Halder, D. (2018). Biodegradable hybrid nanocomposites of chitosan/gelatin and silver nanoparticles for active food packaging applications. *Food Packaging and Shelf Life, 16*, 178–184. https://doi.org/10.1016/j.fpsl.2018.03.008

Li, D., Zhang, L., Song, S., Wang, Z., Kong, C., & Luo, Y. (2017). The role of microorganisms in the degradation of adenosine triphosphate (ATP) in chill-stored common carp (*Cyprinus carpio*) fillets. *Food Chemistry, 224*, 347–352. https://doi.org/10.1016/j.foodchem.2016.12.056

Li, Y., Tang, C., & He, Q. (2021). Effect of orange (*Citrus sinensis* L.) peel essential oil on characteristics of blend films based on chitosan and fish skin gelatin. *Food Bioscience, 41*, Article 100927. https://doi.org/10.1016/j.fbio.2021.100927

Lin, Z., Chen, T., Zhou, L., & Yang, H. (2022). Effect of chlorine sanitizer on metabolic responses of *Escherichia coli* biofilms "big six" during cross-contamination from abiotic surface to sponge cake. *Food Research International, 157*, Article 111361. https://doi.org/10.1016/j.foodres.2022.111361

Liu, Q.-R., Wang, W., Qi, J., Huang, Q., & Xiao, J. (2019). Oregano essential oil loaded soybean polysaccharide films: Effect of Pickering type immobilization on physical and antimicrobial properties. *Food Hydrocolloids, 87*, 165–172. https://doi.org/10.1016/j.foodhyd.2018.08.011

Locci, E., Piras, C., Mereu, S., Cesare Marincola, F., & Scano, P. (2011). 1H NMR metabolite fingerprint and pattern recognition of mullet (*Mugil cephalus*) bottarga. *Journal of Agricultural and Food Chemistry, 59*(17), 9497–9505. https://doi.org/10.1021/jf2012979

Lou, X., Zhai, D., & Yang, H. (2021). Changes of metabolite profiles of fish models inoculated with *Shewanella baltica* during spoilage. *Food Control, 123*, Article 107697. https://doi.org/10.1016/j.foodcont.2020.107697

Martins, J. T., Cerqueira, M. A., & Vicente, A. A. (2012). Influence of α-tocopherol on physicochemical properties of chitosan-based films. *Food Hydrocolloids, 27*(1), 220–227. https://doi.org/10.1016/j.foodhyd.2011.06.011

Moczkowska, M., Półtorak, A., Montowska, M., Pospiech, E., & Wierzbicka, A. (2017). The effect of the packaging system and storage time on myofibrillar protein degradation and oxidation process in relation to beef tenderness. *Meat Science, 130*, 7–15. https://doi.org/10.1016/j.meatsci.2017.03.008

Nisar, T., Wang, Z.-C., Yang, X., Tian, Y., Iqbal, M., & Guo, Y. (2018). Characterization of citrus pectin films integrated with clove bud essential oil: Physical, thermal, barrier, antioxidant and antibacterial properties. *International Journal of Biological Macromolecules, 106*, 670–680. https://doi.org/10.1016/j.ijbiomac.2017.08.068

Pereda, M., Ponce, A. G., Marcovich, N. E., Ruseckaite, R. A., & Martucci, J. F. (2011). Chitosan-gelatin composites and bi-layer films with potential antimicrobial activity. *Food Hydrocolloids, 25*(5), 1372–1381. https://doi.org/10.1016/j.foodhyd.2011.01.001

Pérez Córdoba, L. J., & Sobral, P. J. A. (2017). Physical and antioxidant properties of films based on gelatin, gelatin-chitosan or gelatin-sodium caseinate blends loaded with nanoemulsified active compounds. *Journal of Food Engineering, 213*, 47–53. https://doi.org/10.1016/j.jfoodeng.2017.05.023

Pérez-Córdoba, L. J., Norton, I. T., Batchelor, H. K., Gkatzionis, K., Spyropoulos, F., & Sobral, P. J. A. (2018). Physico-chemical, antimicrobial and antioxidant properties of gelatin-chitosan based films loaded with nanoemulsions encapsulating active compounds. *Food Hydrocolloids, 79*, 544–559. https://doi.org/10.1016/j.foodhyd.2017.12.012

Pilevar, Z., Bahrami, A., Beikzadeh, S., Hosseini, H., & Jafari, S. M. (2019). Migration of styrene monomer from polystyrene packaging materials into foods: Characterization and safety evaluation. *Trends in Food Science & Technology, 91*, 248–261. https://doi.org/10.1016/j.tifs.2019.07.020

Prabhakar, P. K., Vatsa, S., Srivastav, P. P., & Pathak, S. S. (2020). A comprehensive review on freshness of fish and assessment: Analytical methods and recent innovations. *Food Research International, 133*, Article 109157. https://doi.org/10.1016/j.foodres.2020.109157

Ricque-Marie, D., Abdo-de La Parra, M. I., Cruz-Suarez, L. E., Cuzon, G., Cousin, M., & Pike, I. H. (1998). Raw material freshness, a quality criterion for fish meal fed to shrimp. *Aquaculture, 165*(1), 95–109. https://doi.org/10.1016/S0044-8486(98)00229-4

Romero-González, R., Alarcón-Flores, M. I., Vidal, J. L. M., & Frenich, A. G. (2012). Simultaneous determination of four biogenic and three volatile amines in anchovy by ultra-high-performance liquid chromatography coupled to tandem mass spectrometry. *Journal of Agricultural and Food Chemistry, 60*(21), 5324–5329. https://doi.org/10.1021/jf300853p

Roy, S., & Rhim, J.-W. (2021). Fabrication of bioactive binary composite film based on gelatin/chitosan incorporated with cinnamon essential oil and rutin. *Colloids and Surfaces B: Biointerfaces, 204*, Article 111830. https://doi.org/10.1016/j.colsurfb.2021.111830

Scheffler, T., & Gerrard, D. (2007). Mechanisms controlling pork quality development: The biochemistry controlling postmortem energy metabolism. *Meat Science, 77*(1), 7–16. https://doi.org/10.1016/j.meatsci.2007.04.024

Sharif, H. R., Goff, H. D., Majeed, H., Liu, F., Nsor-Atindana, J., Haider, J., Liang, R., & Zhong, F. (2017). Physicochemical stability of β-carotene and α-tocopherol enriched nanoemulsions: Influence of carrier oil, emulsifier and antioxidant. *Colloids and Surfaces A: Physicochemical and Engineering Aspects, 529*, 550–559. https://doi.org/10.1016/j.colsurfa.2017.05.076

Shen, G., Huang, Y., Dong, J., Wang, X., Cheng, K.-K., Feng, J., Xu, J., & Ye, J. (2018). Metabolic effect of dietary taurine supplementation on Nile tilapia (*Oreochromis niloticus*) evaluated by NMR-based metabolomics. *Journal of Agricultural and Food Chemistry, 66*(1), 368–377. https://doi.org/10.1021/acs.jafc.7b03182

Shumilina, E., Ciampa, A., Capozzi, F., Rustad, T., & Dikiy, A. (2015). NMR approach for monitoring post-mortem changes in Atlantic salmon fillets stored at 0 and 4 °C. *Food Chemistry, 184*, 12–22. https://doi.org/10.1016/j.foodchem.2015.03.037

Tessaro, L., Luciano, C. G., Quinta Barbosa Bittante, A. M., Lourenço, R. V., Martelli-Tosi, M., & José do Amaral Sobral, P. (2021). Gelatin and/or chitosan-based films activated with "Pitanga" (*Eugenia uniflora* L.) leaf hydroethanolic extract encapsulated in double emulsion. *Food Hydrocolloids, 113*, Article 106523. https://doi.org/10.1016/j.foodhyd.2020.106523

Wang, H., Ding, F., Ma, L., & Zhang, Y. (2021). Edible films from chitosan-gelatin: Physical properties and food packaging application. *Food Bioscience, 40*, Article 100871. https://doi.org/10.1016/j.fbio.2020.100871

Wang, Y., Li, C., Li, L., Yang, X., Chen, S., Wu, Y., Zhao, Y., Wang, J., Wei, Y., & Yang, D. (2019). Application of UHPLC-Q/TOF-MS-based metabolomics in the evaluation of metabolites and taste quality of Chinese fish sauce (Yu-lu) during fermentation. *Food Chemistry, 296*, 132–141. https://doi.org/10.1016/j.foodchem.2019.05.043

Wu, H., Richards, M. P., & Undeland, I. (2022). Lipid oxidation and antioxidant delivery systems in muscle food. *Comprehensive Reviews in Food Science and Food Safety, 21*(2), 1275–1299. https://doi.org/10.1111/1541-4337.12890

Wu, J., Ge, S., Liu, H., Wang, S., Chen, S., Wang, J., Li, J., & Zhang, Q. (2014). Properties and antimicrobial activity of silver carp (*Hypophthalmichthys molitrix*) skin gelatin-chitosan films incorporated with oregano essential oil for fish preservation. *Food Packaging and Shelf. Life, 2*(1), 7–16. https://doi.org/10.1016/j.fpsl.2014.04.004

Yadav, S., Mehrotra, G. K., Bhartiya, P., Singh, A., & Dutta, P. K. (2020). Preparation, physicochemical and biological evaluation of quercetin based chitosan-gelatin film for food packaging. *Carbohydrate Polymers, 227*, Article 115348. https://doi.org/10.1016/j.carbpol.2019.115348

Yang, C., Tang, H., Wang, Y., Liu, Y., Wang, J., Shi, W., & Li, L. (2019). Development of PLA-PBSA based biodegradable active film and its application to salmon slices. *Food Packaging and Shelf Life, 22*, Article 100393. https://doi.org/10.1016/j.fpsl.2019.100393

Yemmireddy, V. K., Cason, C., Moreira, J., & Adhikari, A. (2020). Effect of pecan variety and the method of extraction on the antimicrobial activity of pecan shell extracts against different foodborne pathogens and their efficacy on food matrices. *Food Control, 112*, Article 107098. https://doi.org/10.1016/j.foodcont.2020.107098

Yongsawatdigul, J., Choi, Y. J., & Udomporn, S. (2004). Biogenic amines formation in fish sauce prepared from fresh and temperature-abused Indian anchovy (*Stolephorus indicus*). FCT312-FCT319 *Journal of Food Science, 69*(4). https://doi.org/10.1111/j.1365-2621.2004.tb06333.x.

Zhang, C., Yang, Z., Shi, J., Zou, X., Zhai, X., Huang, X., Li, Z., Holmes, M., Daglia, M., & Xiao, J. (2021). Physical properties and bioactivities of chitosan/gelatin-based films loaded with tannic acid and its application on the preservation of fresh-cut apples. *LWT - Food Science and Technology, 144*, Article 111223. https://doi.org/10.1016/j.lwt.2021.111223

Zhao, X., Chen, L., Wu, J. e, He, Y., & Yang, H. (2020). Elucidating antimicrobial mechanism of nisin and grape seed extract against *Listeria monocytogenes* in broth and on shrimp through NMR-based metabolomics approach. *International Journal of Food Microbiology, 319*, Article 108494. https://doi.org/10.1016/j.ijfoodmicro.2019.108494

Zhao, X., Wu, J. e, Chen, L., & Yang, H. (2019). Effect of vacuum impregnated fish gelatin and grape seed extract on metabolite profiles of tilapia (*Oreochromis niloticus*) fillets during storage. *Food Chemistry, 293*, 418–428. https://doi.org/10.1016/j.foodchem.2019.05.001